CT Coronary Angiography: 256-Slice and 320-Detector Row Scanners

Edward M. Hsiao, **Frank J. Rybicki**, and **Michael Steigner**
Applied Imaging Science Laboratory, Brigham and Women's Hospital Radiology & Harvard Medical School, 75 Francis Street, Boston, MA 02115, USA

Frank J. Rybicki: frybicki@partners.org

Abstract

Multidetector computed tomography (MDCT) has rapidly evolved from 4-detector row systems in 1998 to 256-slice and 320-detector row CT systems. With smaller detector element size and faster gantry rotation speed, spatial and temporal resolution of the 64-detector MDCT scanners have made coronary artery imaging a reliable clinical test. Wide-area coverage MDCT, such as the 256-slice and 320-detector row MDCT scanners, has enabled volumetric imaging of the entire heart free of stair-step artifacts at a single time point within one cardiac cycle. It is hoped that these improvements will be realized with greater diagnostic accuracy of CT coronary angiography. Such scanners hold promise in performing a rapid high quality "triple rule-out" test without high contrast load, improved myocardial perfusion imaging, and even four-dimensional CT subtraction angiography. These emerging technical advances and novel applications will continue to change the way we study coronary artery disease beyond detecting luminal stenosis.

Keywords

Computed tomography; Coronary artery disease; Wide area detector; Imaging; Technology

Introduction

This article highlights the role of wide-area detector CT for cardiac imaging. Technical specifications of the hardware are described, as are novel potential clinical applications.

Nomenclature of MDCT

Single-source multidetector computed tomography (MDCT) uses a single x-ray source mounted opposite to a detector array. The x-ray tube and detector array system rotates around the patient to generate tomographic images. To reconstruct a transverse CT image, the gantry requires a rotation of approximately 180°. Dual-source CT uses two x-ray tubes with opposing detector arrays mounted 90° from each other. The main advantage of this system is that the temporal resolution is effectively halved because each x-ray tube/detector array system only needs to rotate half of the angle that would otherwise be required by a single-source system.

The number of detector rows in the longitudinal axis (z-axis) and the number of slices of an MDCT system are not interchangeable terms because multiple systems with an alternating focal spot allow the same z-axis coverage to be sampled twice, and thus the number of image

slices generated is double the number of detector rows. However, the volume coverage (ie, z-axis coverage) remains the same; for example, a 128-detector row scanner with two alternating z-focal spot positions can be referred to as 256-slice CT. It is important to specify the number of detector rows in z-axis, with or without alternating focal spot positions, and single versus dual source.

Development in CT Coronary Angiography

CT coronary angiography became clinically practical with retrospective electrocardiogram (ECG) gating to freeze cardiac motion plus the z-axis coverage from 16-detector row scanners [1]. Following 16-detector row technology, the clinical accuracy of MDCT in coronary artery disease (CAD) detection is now recognized by two multicenter trials based on 64-detector row, single-source, single focal spot MDCT. The ACCURACY (Assessment by Coronary Computed Tomographic Angiography of Individuals Undergoing Invasive Coronary Angiography) trial based in the United States demonstrated the sensitivity, specificity, positive predictive values (PPVs), and negative predictive values (NPVs) for greater than 50% stenosis to be 0.95, 0.83, 0.64, and 0.99, respectively, on a per-patient basis [2••]. The Core-64 multicenter trial subsequently showed the sensitivity, specificity, PPV, and NPV of 085, 0.90, 0.91, and 0.83, respectively [3••]. The slightly lower than expected NPV for Core-64 can be at least partly attributed to the high prevalence of obstructive CAD (56%) in the study population. The 2006 American College of Cardiology appropriateness guidelines considered the use of MDCT as an appropriate indication to exclude CAD in low- and intermediate-risk individuals [4].

Using those systems tested in the multicenter trials, cardiac motion artifacts, stair-step artifacts, and small vessel diameter less than 1.5 mm render around 20% of the coronary segments uninterpretable [3••,5]. Heavily calcified vessels and coronary stents also impose diagnostic challenges. In the "post-64" era, the MDCT technology started branching out in various directions to overcome these limitations. The first direction is to increase the number of detector elements and, therefore, the volume coverage along the z-axis of detector block. The second is to increase sensitivity of detector material. Next is the use of iterative image reconstruction algorithms [6,7]. The last are dual-source CT [8,9] scanners that use a high-pitch acquisition strategy [10] to capture the entire heart within one heartbeat. To date, most new technology developments are available only on different systems, although they may be combined in future CT releases.

State-of-the-Art Wide-Coverage MDCT Scanners

320-Detector Row, Single-Source, Single Focal Spot

This hardware (Aquilion One Dynamic Volume CT; Toshiba Medical System, Tochigi-ken, Japan) currently has the largest z-axis detector coverage. It was released shortly after experiments with a 256-detector row MDCT prototype [11–14]. Each detector element is 0.5 mm wide, yielding a maximum of 16-cm z-axis coverage. This configuration allows three-dimensional volumetric wholeheart imaging during the diastole of one R-R interval. In 320-detector row CT, the entire heart is imaged with temporal uniformity (ie, at the same time point without temporal delay from the base to apex). Furthermore, if the x-ray beam is turned on for a longer period, the scanner can capture the heart over one or more cardiac cycles. This has been described as four-dimensional CT or volumetric cine imaging [14].

The temporal resolution of an MDCT scanner reflects the ability to freeze cardiac motion, thus producing motion-free images. The 320-detector scanner has a standard temporal resolution of approximately 175 ms, one half the gantry rotation time. This remains significantly longer than the 33 ms of catheter coronary angiography operating at 30 frames per second. Therefore,

to achieve excellent image quality, meticulous heart rate control is mandatory. Coronary opacification gradients are linked to blood flow and fractional flow reserve, and may have implications particularly for patients with indeterminate lesions, or for patients with diffuse CAD without focal stenosis [15]. In the latter case, a graded, continuous pressure drop along the arterial length results in flow resistance. In diffuse CAD, the lumen area is diffusely smaller than normal, and thus there is no reference segment for qualitative measurements for visual assessment.

For patients with higher heart rate (>65 bpm) and contraindications to β blockers, multisegment reconstruction can be used at the expense of higher radiation dose. For example, in two-segment reconstruction, data required for image reconstruction are acquired over two cardiac cycles. Therefore, only data from 90° rotation during each of the two cardiac cycles are used, improving the effective temporal resolution by a factor of 2.

128-Detector Row, Single-Source, Dual Focal Spot

At the November 2007 annual meeting of the Radiological Society of North America, Philips introduced the 256-slice MDCT (Brilliance iCT; Philips Healthcare, Cleveland, OH), a 128×0.625-mm detector row system with dual focal spot positions to double the number of slices within the 8-cm (width) z-axis gantry coverage. The iCT has 270-ms gantry rotation time, which translates to an approximate temporal resolution of 135 ms. Prospectively ECG-gated cardiac CT typically covers the entire heart in two axial acquisitions over three heartbeats. During the diastole of the first heartbeat, the upper half of the heart is imaged. During the second heartbeat, the patient table translates 62.4 mm. Subsequently, the lower half of the heart is acquired during the diastole of the third heartbeat. The scanner is equipped with several radiation reduction capabilities, including a dynamic helical collimator and an adaptive axial collimator to reduce z-overscanning [16,17].

64-Detector Row, Dual-Source, Dual Focal Spot

The second-generation dual-source MDCT (Somatom Definition FLASH; Siemens Medical Solution, Forchheim, Germany) introduced at the end of 2008 is equipped with two 64-detector row units, each with an alternating focal spot. The 360° gantry rotation time is 280 ms, translating to a temporal resolution of approximately 75 ms when the scanner operates with both x-ray tubes collecting data at the same energy. The vendor has proposed a high-pitch prospectively gated scanning acquisition. In single-source MDCT, the maximum pitch is roughly 1.5 for gapless image reconstruction. The pitch can be increased up to 3.2 in dual-source systems. For coronary CT angiography, the typical phase window required for a diagnostic quality examination regarding motion artifact is 10% of the R-R interval [18]. The pitch required for multiphase acquisition ranges from 0.2 to 0.5 (depending on the heart rate). With the high-pitch acquisition mode, only one "phase" is acquired, which gradually increases with the z-axis table translation (ie, the phase at the top of the scan range is different and earlier than the phase acquired at the bottom of the scan range). The influence on image quality for different clinical scenarios and heart rates will be evaluated with second-generation dual-source MDCT. Achenbach et al. [10] recently demonstrated the feasibility of this new scanning method using first-generation dual-source CT. Slow and regular heart rates are the prerequisites for this acquisition that is prospectively triggered by ECG and is anticipated to scan the entire heart (12 cm) in 270 ms, with a pitch of 3.2 [10].

Another potential advantage of dual-source CT is tissue characterization with both detector systems operating at different kilovolts, so-called "dual-energy CT" [19]. Although this has not been clinically realized to date, two x-ray beams of different energy spectra in theory could better demonstrate varying attenuation characteristics of different tissues [20,21••]. In this approach the temporal resolution is sacrificed, and scanning requires a larger number of

subvolumes, or slabs. In the case of differentiating myocardial perfusion defects from normal myocardium [19,20,22], this will likely be problematic because the scan time can extend to over 5 s.

Advantages

Elimination of Stair-Step and Misalignment Artifacts

Larger detector row widths limit the number of subvolumes, or slabs, needed for cardiac CT, with the limit of z-axis coverage as 16 cm. For this technology, axial CT cardiac acquisitions eliminate artifacts inherent in subvolume imaging over several cardiac cycles. An initial report of 40 patients using this method showed that 89% and 99% of all coronary segments were of excellent and diagnostic quality, respectively. The effective dose ranged from 4.9 to 9.4 mSv with prospective ECG gating, and 60% to 100% phase window in one cardiac cycle acquisition [21••].

Lowering Radiation Dose

Increasing the number of detector rows in an MDCT scanner generally increases radiation dose to patients. However, shorter scanning time, elimination of redundant radiation from helical oversampling, or overlapping of sequential axial acquisitions translate to lower than expected radiation dose despite the higher number of detector rows in these wide-coverage MDCT scanners. Early 4-detector coronary CT angiograms reported patient doses of 3.9 to 5.8 mSv [23]. Using retrospective ECG gating on a 64-detector single-source CT had doses near 18.4 mSv, with a range from 15 to 21 mSv [3••,24–26•]. With ECG-controlled tube current modulation, the average dose can be reduced to 9.4 mSv for 64-detector MDCT [27,28•]. Prospective ECG gating allows the x-ray beams to be turned on during preselected phases in the cardiac cycles, and has been shown by various studies to further reduce radiation dose by 52% to 85% [17,21••,29–31•,32–36•] while maintaining equivalent diagnostic accuracy compared with retrospective scanning [31•,35,37••,38].

The initial experience with 128×2 detector row CT showed a mean effective dose of 4 mSv, ranging from 2.1 to 7.0 mSv [39]. The initial experience with 320-detector row CT had a mean effective dose of 7.2 mSv, ranging from 4.9 to 16.5 mSv [21••], with reductions based on careful selection of phase window and modification of x-ray output based on the patient's body habitus.

Reduced Intravenous Contrast Requirement

With rapid volumetric coverage, the duration of vascular contrast opacification required for image acquisition is significantly reduced. In patients with normal cardiac output, some have reported the contrast volume for CT coronary angiogram can be as low as 45 mL at 5 mL/sec [39]. This could benefit patients with renal impairment and decrease the risk of contrast-induced nephropathy.

Applications Beyond Coronary CT Angiography

Volumetric Myocardial Imaging for Function, Perfusion, and Viability

Volumetric imaging using wide-area coverage scanners can acquire data from the cardiac apex to the base with minimal, or in the limit of 16-cm z-axis coverage, no time delay. For functional assessment, the left ventricle ejection fraction (LVEF) is calculated with the x-ray beam evaluating a single cardiac cycle from end systole to end diastole. The radiation dose for such a protocol using a wide-area detector scanner is estimated to be 4 to 12 mSv with 60 to 80 mL of contrast [5]. This method estimates the end-systolic and end-diastolic volumes and thus the

LVEF. However, the effects of shunting, aortic or mitral valve regurgitation cannot be assessed as is available using echocardiography and cardiac MRI.

Because iodinated contrast has similar extracellular kinetics to gadolinium contrast used in MRI [40], several early studies [40,41••,42–46] have performed first-pass myocardial perfusion imaging and/or delayed contrast enhancement using 16-, single-source 64-detector row, or 32×2 dual-source CT to detect myocardial infarct or scar. Myocardial scar is characterized by hyperenhancement on delayed imaging (>10 min after contrast administration) and does not require rapid data acquisition. For perfusion imaging, fast imaging techniques and temporal resolution are important to capture the first pass of contrast in the myocardium. Although further investigation is required, rapid volumetric imaging with temporal uniformity will likely help delineate small or subtle perfusion defects by allowing comparison of the abnormally perfused myocardium to normal myocardium imaged at the same time point.

Early experiments reported that coronary imaging, functional assessment, and rest and stress myocardial perfusion can be achieved over three to five heartbeats with 14 to 16 mSv as an effective dose and 120 to 140 mL of contrast [5]. The stress perfusion is a pharmacologic test, and high temporal resolution is important because the heart rate will be increased from the resting state of 60 to 70 bpm. Selection of an agent with less chronotropic effect is desirable and the use of a multisegmented approach can improve the temporal resolution and the signal-to-noise ratio at the expense of a higher radiation dose.

Evaluation for Acute Chest Pain and "Triple Rule-Out" Test

In the 2006 National Health Statistics Report, acute chest pain accounted for over 6 million emergency department visits and close to 2 million hospital admissions in the United States [47]. Patients with suspected acute coronary syndrome routinely undergo serial ECG, serial troponin tests, and stress tests with prolonged emergency department stays or admissions. The health care cost is estimated to be more than $8 billion per year, of which $6 billion is spent on negative cardiac evaluation [48•].

Studies have shown that coronary CT using 64-detector row single-source, single focal spot CT is a safe and efficient method to triage patients with acute chest pain who have a low to intermediate likelihood of CAD due to its high NPV, diagnostic efficacy, time efficiency, and cost-effectiveness [49,50•,51•]. A negative study or result with clinically insignificant stenosis (≤ 50%) in these patients can lead to prompt exclusion of acute coronary syndrome. Complex plaques with high-risk features or severe coronary artery stenosis on CT can expedite patients to invasive coronary angiography. Patients with an intermediate (50% to 70%) degree of stenosis by should undergo further testing, such as a conventional nuclear stress. In addition, approximately 10% of the CT evaluations are inconclusive or nondiagnostic (retrospective ECG gating 64-detector row single-source, single focal spot) [50•,51•]. Wider detector coverage can potentially decrease stair-step and misalignment artifacts leading to a lower number of inconclusive or nondiagnostic studies.

Several "triple rule-out" protocols have been proposed to provide high-quality images covering the thoracic aorta, coronary, and pulmonary arterial trees. The examination must be able to exclude life-threatening conditions, including pulmonary embolism, aortic dissection, and acute coronary syndrome, among patients with acute chest pain and low to intermediate risk of acute coronary syndrome. These protocols remain challenging because of 1) limited ability of subvolume MDCT scanners to rapidly cover a large volume (at least from aortic arch to cardiac inferior wall); 2) the requirement of large volume iodine contrast; and 3) high radiation dose.

Hein et al. [52] exploited the wide-area coverage of a 320-detector row scanner and performed a triple rule-out protocol in 30 patients. The protocol included three axial nongated volume acquisitions to cover the chest with triggering at the pulmonary arteries followed by a prospectively ECG-gated cardiac scan for the coronary arteries. Both phases used 45 mL of iodinated contrast respectively. The average effective radiation dose was 7 to 9 mSv for heart rates less than 65 bpm (ie, single-segment image reconstruction for the coronary scan).

Endothelial Shear Stress and Coronary Vascular Profiling

Endothelial shear stress (ESS) is the frictional force exerted on the endothelial surface by the blood flowing through the artery. ESS is determined by geometric variations of the coronary anatomy as it courses around the heart. Low ESS (<0.5 Pa) is known to predispose the development and progression of atherosclerotic plaque. Such change culminates in high-risk vulnerable plaque, which is likely to rupture and cause acute coronary events [53••]. Currently, "vascular profiling" of the entire length of a coronary artery is performed invasively using intravascular ultrasound and catheter angiography to recreate the individual coronary lumen [54]. This is followed by simulations of the blood flow in the coronary artery using computational fluid dynamics. The methodology can provide accurate assessment of local hemodynamic forces, such as ESS, and the local plaque size, morphology, and tissue characterization. However, the invasive nature of the test limits its widespread use.

Early noninvasive identification of low ESS coronary artery segments at risk would be invaluable for risk stratification and coronary event prevention. It has been proposed that highly selective interventions to segments at risk could prevent future cardiac events. Early attempts at performing CT-derived shear stress maps from fluid dynamic simulations have used subvolume CT scanners that are prone to various artifacts leading to limited precision in determining coronary anatomy and distorted coronary hemodynamics [55]. High-quality single-heartbeat volumetric CT coronary angiography presents significant potential in the noninvasive assessment of ESS (Fig. 1) [56].

Cine Volumetric Imaging and Four-Dimensional Subtraction Angiography

With volumetric cine scanning mode, it is feasible to perform CT subtraction angiography. Having the x-ray beam being turned on throughout numerous gantry rotations without ECG gating, dynamic CT angiographic images can be acquired by reconstructing transverse source images and subsequently three-dimensional reformats at very short time intervals (eg, 0.1 s). Continuous imaging over a large volume without patient table motion allows more accurate subtraction of background from angiographic phase images. However, the first challenge for this application is the huge dataset (320 slices×10 frames/sec) that can cause significant delay in the calculation time (up to 76 min in an animal model with 256-detector MDCT prototype) [57•]. A raw data-based subtraction method has been developed; therefore, image subtraction can be performed with manipulation of raw data before completing image reconstruction with filtered back projection [14,57•]. The second challenge is cardiac motion that makes this technique more difficult than in the central nervous system vasculature [58].

Coronary Artery Opacification Gradients

As opposed to invasive catheterization, CT does not have a direct means to measure coronary pressure changes. A novel application of wide-area coverage cardiac CT may extend beyond anatomic plaque assessment by capitalizing on the temporal uniformity of the acquired images by measuring contrast opacification (density) gradient across atherosclerotic lesions.

Initial experiences have shown that Hounsfield unit (HU) measurements near coronary ostia were greater than those measured distally [21••]. A follow-up study demonstrated statistically larger gradient change of contrast density across stenotic lesions [15]. For example, the

difference in HU between the ostium and where an angiographically normal artery tapers to 2.5 mm was approximately 39 HU (*n*=84 arteries). This difference increased to 55 HU higher in arteries with greater than 20% stenosis.

Furthermore, the contrast gradient within a coronary artery has been shown to be gradual along the length of the artery. The contrast concentration at any point of an end artery is intrinsically related to the cumulative resistance to the flow of contrast-opacified blood up to that location. Thus, contrast opacification gradient between two points in the artery may carry information related to flow characteristics. It may be that coronary opacification gradients are linked to blood flow and fractional flow reserve, and may have implications particularly for patients with indeterminate lesions, or for patients with diffuse CAD without focal stenosis. In the latter case, a graded, continuous pressure drop along the arterial length results in flow resistance. In diffuse CAD the lumen area is diffusely smaller than normal, and thus there is no reference segment for qualitative measurements for visual assessment.

Conclusions

In the "post-64 era," MDCT technology has branched into wide-area detector coverage and dual-source acquisition strategies. Both directions of evolution have different potentials and clinical applications. Beyond the elimination of helical and stair-step artifacts, new technologies are one step closer to a more comprehensive cardiac evaluation. It is likely that wide-area coverage and dual-source technology will not remain mutually exclusive with further technology improvements.

References

Papers of particular interest, published recently, have been highlighted as:

• Of importance

•• Of major importance

1. Lawler LP, Pannu HK, Fishman EK. MDCT evaluation of the coronary arteries, 2004: how we do it —data acquisition, postprocessing, display, and interpretation. AJR Am J Roentgenol 2005;184:1402–1412. [PubMed: 15855087]

2••. Budoff M, Dowe D, Jollis J, et al. Diagnostic performance of 64-multidetector row coronary computed tomographic angiography for evaluation of coronary artery stenosis in individuals without known coronary artery disease: results from the prospective multicenter ACCURACY (Assessment by Coronary Computed Tomographic Angiography of Individuals Undergoing Invasive Coronary Angiography) trial. J Am Coll Cardiol 2008;52:1724–1732. This is a major trial in the diagnostic accuracy of 64-MDCT CT coronary angiography. [PubMed: 19007693]

3•• . Miller JM, Rochitte CE, Dewey M, et al. Diagnostic performance of coronary angiography by 64-row CT. N Engl J Med 2008;359:2324–2336. This is another major trial in the diagnostic accuracy of 64-MDCT CT coronary angiography. [PubMed: 19038879]

4. American College of Radiology; Society of Cardiovascular Computed Tomography; Society for Cardiovascular Magnetic Resonance; American Society of Nuclear Cardiology; North American Society for Cardiac Imaging; Society for Cardiovascular Angiography and Interventions; Society of Interventional Radiology. ACCF/ACR/SCCT/SCMR/ASNC/NASCI/SCAI/SIR 2006 appropriateness criteria for cardiac computed tomography and cardiac magnetic resonance imaging. A report of the American College of Cardiology Foundation Quality Strategic Directions Committee Appropriateness Criteria Working Group. J Am Coll Radiol 2006;3:751–771. [PubMed: 17412166]

5. Voros S. What are the potential advantages and disadvantages of volumetric CT scanning? J Cardiovasc Comput Tomogr 2009;3:67–70. [PubMed: 19201673]

6. Hara AK, Paden RG, Silva AC, et al. Iterative reconstruction technique for reducing body radiation dose at CT: feasibility study. AJR Am J Roentgenol 2009;193:764–771. [PubMed: 19696291]

7. Min JK, Swaminathan RV, Vass M, et al. High-definition multidetector computed tomography for evaluation of coronary artery stents: comparison to standard-definition 64-detector row computed tomography. J Cardiovasc Comput Tomogr 2009;3:246–251. [PubMed: 19577213]

8. Achenbach S, Ropers D, Kuettner A, et al. Contrast-enhanced coronary artery visualization by dual-source computed tomography—initial experience. Eur J Radiol 2006;57:331–335. [PubMed: 16426789]

9. Dey D, Lee CJ, Ohba M, et al. Image quality and artifacts in coronary CT angiography with dual-source CT: initial clinical experience. J Cardiovasc Comput Tomogr 2008;2:105–114. [PubMed: 19083930]

10. Achenbach S, Marwan M, Schepis T, et al. High-pitch spiral acquisition: a new scan mode for coronary CT angiography. J Cardiovasc Comput Tomogr 2009;3:117–121. [PubMed: 19332343]

11. Kido T, Kurata A, Higashino H, et al. Cardiac imaging using 256-detector row four-dimensional CT: preliminary clinical report. Radiat Med 2007;25:38–44. [PubMed: 17225052]

12. Mori S, Endo M, Obata T, et al. Clinical potentials of the prototype 256-detector row CT-scanner. Acad Radiol 2005;12:148–154. [PubMed: 15721591]

13. Mori S, Endo M, Obata T, et al. Properties of the prototype 256-row (cone beam) CT scanner. Eur Radiol 2006;16:2100–2108. [PubMed: 16568264]

14. Mori S, Kondo C, Suzuki N, et al. Volumetric cine imaging for cardiovascular circulation using prototype 256-detector row computed tomography scanner (4-dimensional computed tomography): a preliminary study with a porcine model. J Comput Assist Tomogr 2005;29:26–30. [PubMed: 15665678]

15. Steigner ML, Mitsouras D, Whitmore AG, et al. Iodinated contrast opacification gradients in normal coronary arteries imaged with prospectively ECG-gated single heart beat 320-detector row computed tomography. Circulation Cardiovascular Imaging. 2010 in press.

16. Hameed T, Teague S, Vembar M, et al. Low radiation dose ECG-gated chest CT angiography on a 256-slice multidetector CT scanner. Int J Cardiovasc Imaging 2009;25:267–278.

17. Walker M, Olszewski M, Desai M, et al. New radiation dose saving technologies for 256-slice cardiac computed tomography angiography. Int J Cardiovasc Imaging 2009;25:189–199.

18. Steigner ML, Otero HJ, Cai T, et al. Narrowing the phase window width in prospectively ECG-gated single heart beat 320-detector row coronary CT angiography. Int J Cardiovasc Imaging 2009;25:85–90. [PubMed: 18663599]

19. Schwarz F, Ruzsics B, Schoepf UJ, et al. Dual-energy CT of the heart—principles and protocols. Eur J Radiol 2008;68:423–433. [PubMed: 19008064]

20. Ruzsics B, Lee H, Zwerner PL, et al. Dual-energy CT of the heart for diagnosing coronary artery stenosis and myocardial ischemia-initial experience. Eur Radiol 2008;18:2414–2424. [PubMed: 18523782]

21••. Rybicki FJ, Otero HJ, Steigner ML, et al. Initial evaluation of coronary images from 320-detector row computed tomography. Int J Cardiovasc Imaging 2008;24:535–546. This is the first published clinical experience based on the 320-detector row MDCT system. [PubMed: 18368512]

22. Ruzsics B, Lee H, Powers ER, et al. Images in cardiovascular medicine. Myocardial ischemia diagnosed by dual-energy computed tomography: correlation with single-photon emission computed tomography. Circulation 2008;117:1244–1245. [PubMed: 18316501]

23. Achenbach S, Ropers D, Möhlenkamp S, et al. Variability of repeated coronary artery calcium measurements by electron beam tomography. Am J Cardiol 2001;87:210–213. A8. [PubMed: 11152842]

24. Budoff M, Achenbach S, Blumenthal R, et al. Assessment of coronary artery disease by cardiac computed tomography: a scientific statement from the American Heart Association Committee on Cardiovascular Imaging and Intervention, Council on Cardiovascular Radiology and Intervention, and Committee on Cardiac Imaging, Council on Clinical Cardiology. Circulation 2006;114:1761–1791. [PubMed: 17015792]

25. Mollet NR, Cademartiri F, van Mieghem CA, et al. High-resolution spiral computed tomography coronary angiography in patients referred for diagnostic conventional coronary angiography. Circulation 2005;112:2318–2323. [PubMed: 16203914]

26• . Einstein AJ, Henzlova MJ, Rajagopalan S. Estimating risk of cancer associated with radiation exposure from 64-slice computed tomography coronary angiography. JAMA 2007;298:317–323. This is an excellent discussion of radiation dose from coronary CT angiography. [PubMed: 17635892]

27. Hausleiter J, Meyer T, Hadamitzky M, et al. Radiation dose estimates from cardiac multislice computed tomography in daily practice: impact of different scanning protocols on effective dose estimates. Circulation 2006;113:1305–1310. [PubMed: 16520411]

28• . Einstein A, Moser K, Thompson R, et al. Radiation dose to patients from cardiac diagnostic imaging. Circulation 2007;116:1290–1305. This is another excellent discussion of radiation dose from coronary CT angiography. [PubMed: 17846343]

29. Earls JP, Berman EL, Urban BA, et al. Prospectively gated transverse coronary CT angiography versus retrospectively gated helical technique: improved image quality and reduced radiation dose. Radiology 2008;246:742–753. [PubMed: 18195386]

30. Gutstein A, Wolak A, Lee C, et al. Predicting success of prospective and retrospective gating with dual-source coronary computed tomography angiography: development of selection criteria and initial experience. J Cardiovasc Comput Tomogr 2008;2:81–90. [PubMed: 19083926]

31• . Hirai N, Horiguchi J, Fujioka C, et al. Prospective versus retrospective ECG-gated 64-detector coronary CT angiography: assessment of image quality, stenosis, and radiation dose. Radiology 2008;248:424–430. This is a comparison between prospective and retrospective ECG gating. [PubMed: 18574140]

32. Hsieh J, Londt J, Vass M, et al. Step-and-shoot data acquisition and reconstruction for cardiac x-ray computed tomography. Med Phys 2006;33:4236–4248. [PubMed: 17153402]

33. Husmann L, Valenta I, Gaemperli O, et al. Feasibility of low-dose coronary CT angiography: first experience with prospective ECG-gating. Eur Heart J 2008;29:191–197. [PubMed: 18089704]

34. Klass O, Jeltsch M, Feuerlein S, et al. Prospectively gated axial CT coronary angiography: preliminary experiences with a novel low-dose technique. Eur Radiol 2009;19:829–836. [PubMed: 19011864]

35. Scheffel H, Alkadhi H, Leschka S, et al. Low-dose CT coronary angiography in the step-and-shoot mode: diagnostic performance. Heart 2008;94:1132–1137. [PubMed: 18519548]

36• . Shuman WP, Branch KR, May JM, et al. Prospective versus retrospective ECG gating for 64-detector CT of the coronary arteries: comparison of image quality and patient radiation dose. Radiology 2008;248:431–437. This is another comparison between prospective and retrospective ECG gating. [PubMed: 18552312]

37••. Pontone G, Andreini D, Bartorelli AL, et al. Diagnostic accuracy of coronary computed tomography angiography: a comparison between prospective and retrospective electrocardiogram triggering. J Am Coll Cardiol 2009;54:346–355. This is another comparison between prospective and retrospective ECG gating. [PubMed: 19608033]

38. Stolzmann P, Leschka S, Scheffel H, et al. Dual-source CT in step-and-shoot mode: noninvasive coronary angiography with low radiation dose. Radiology 2008;249:71–80. [PubMed: 18796669]

39. Weigold W, Olszewski M, Walker M. Low-dose prospectively gated 256-slice coronary computed tomographic angiography. Int J Cardiovasc Imaging 2009;25:217–230.

40. Gerber BL, Belge B, Legros GJ, et al. Characterization of acute and chronic myocardial infarcts by multidetector computed tomography: comparison with contrast-enhanced magnetic resonance. Circulation 2006;113:823–833. [PubMed: 16461822]

41•• . Cury RC, Nieman K, Shapiro MD, et al. Comprehensive assessment of myocardial perfusion defects, regional wall motion, and left ventricular function by using 64-section multidetector CT. Radiology 2008;248:466–475. This paper discusses the use of MDCT in myocardial perfusion. [PubMed: 18641250]

42. Lessick J, Dragu R, Mutlak D, et al. Is functional improvement after myocardial infarction predicted with myocardial enhancement patterns at multidetector CT? Radiology 2007;244:736–744. [PubMed: 17690323]

43. Nieman K, Cury RC, Ferencik M, et al. Differentiation of recent and chronic myocardial infarction by cardiac computed tomography. Am J Cardiol 2006;98:303–308. [PubMed: 16860013]

44. Nieman K, Shapiro MD, Ferencik M, et al. Reperfused myocardial infarction: contrast-enhanced 64-Section CT in comparison to MR imaging. Radiology 2008;247:49–56. [PubMed: 18372464]

45. Nikolaou K, Sanz J, Poon M, et al. Assessment of myocardial perfusion and viability from routine contrast-enhanced 16-detector-row computed tomography of the heart: preliminary results. Eur Radiol 2005;15:864–871. [PubMed: 15776243]

46. Rubinshtein R, Miller TD, Williamson EE, et al. Detection of myocardial infarction by dual-source coronary computed tomography angiography using quantitated myocardial scintigraphy as the reference standard. Heart 2009;95:1419–1422. [PubMed: 19196731]

47. Pitts SR, Niska RW, Xu J, Burt CW. National Hospital Ambulatory Medical Care Survey: 2006 emergency department summary. Natl Health Stat Report 2008;6:1–38. [PubMed: 18839799]

48• . Rubinshtein R, Halon DA, Gaspar T, et al. Usefulness of 64-slice cardiac computed tomographic angiography for diagnosing acute coronary syndromes and predicting clinical outcome in emergency department patients with chest pain of uncertain origin. Circulation 2007;115:1762–1768. This paper discusses the use of CT coronary angiography in emergency departments. [PubMed: 17372178]

49. Chang SA, Choi SI, Choi EK, et al. Usefulness of 64-slice multidetector computed tomography as an initial diagnostic approach in patients with acute chest pain. Am Heart J 2008;156:375–383. [PubMed: 18657674]

50• . Goldstein JA, Gallagher MJ, O'Neill WW, et al. A randomized controlled trial of multi-slice coronary computed tomography for evaluation of acute chest pain. J Am Coll Cardiol 2007;49:863–871. This paper also discusses the use of CT coronary angiography in emergency departments. [PubMed: 17320744]

51• . Hoffmann U, Bamberg F, Chae C, et al. Coronary computed tomography angiography for early triage of patients with acute chest pain. J Am Coll Cardiol 2009;53:1642–1650. This paper also discusses the use of CT coronary angiography in emergency departments. [PubMed: 19406338]

52. Hein PA, Romano VC, Lembcke A, et al. Initial experience with a chest pain protocol using 320-slice volume MDCT. Eur Radiol 2009;19:1148–1155. [PubMed: 19137311]

53••. Chatzizisis YS, Jonas M, Coskun AU, et al. Prediction of the localization of high-risk coronary atherosclerotic plaques on the basis of low endothelial shear stress: an intravascular ultrasound and histopathology natural history study. Circulation 2008;117:993–1002. This paper discusses an innovative noninvasive approach to measure endothelial shear stress. [PubMed: 18250270]

54. Coskun AU, Yeghiazarians Y, Kinlay S, et al. Reproducibility of coronary lumen, plaque, and vessel wall reconstruction and of endothelial shear stress measurements in vivo in humans. Catheter Cardiovasc Interv 2003;60:67–78. [PubMed: 12929106]

55. Frauenfelder T, Boutsianis E, Schertler T, et al. In-vivo flow simulation in coronary arteries based on computed tomography datasets: feasibility and initial results. Eur Radiol 2007;17:1291–1300. [PubMed: 17061068]

56. Rybicki FJ, Melchionna S, Mitsouras D, et al. Prediction of coronary artery plaque progression and potential rupture from 320-detector row prospectively ECG-gated single heart beat CT angiography: Lattice Boltzmann evaluation of endothelial shear stress. Int J Cardiovasc Imaging 2009;25:289–299. [PubMed: 19043805]

57• . Mori S, Endo M. Candidate image processing for real-time volumetric CT subtraction angiography. Eur J Radiol 2007;61:335–341. This paper discusses the potential use of wide coverage area MDCT in performing four-dimensional CT subtraction angiography. [PubMed: 17097254]

58. Yahyavi-Firouz-Abadi N, Wynn BL, Rybicki FJ, et al. Steroid-responsive large vessel vasculitis: application of whole-brain 320-detector row dynamic volume CT angiography and perfusion. AJNR Am J Neuroradiol 2009;30:1409–1411. [PubMed: 19556352]

59. Ramkumar PG, Mitsouras D, Feldman CL, et al. New advances in cardiac computed tomography. Curr Opin Cardiol 2009;24:596–603. [PubMed: 19752727]
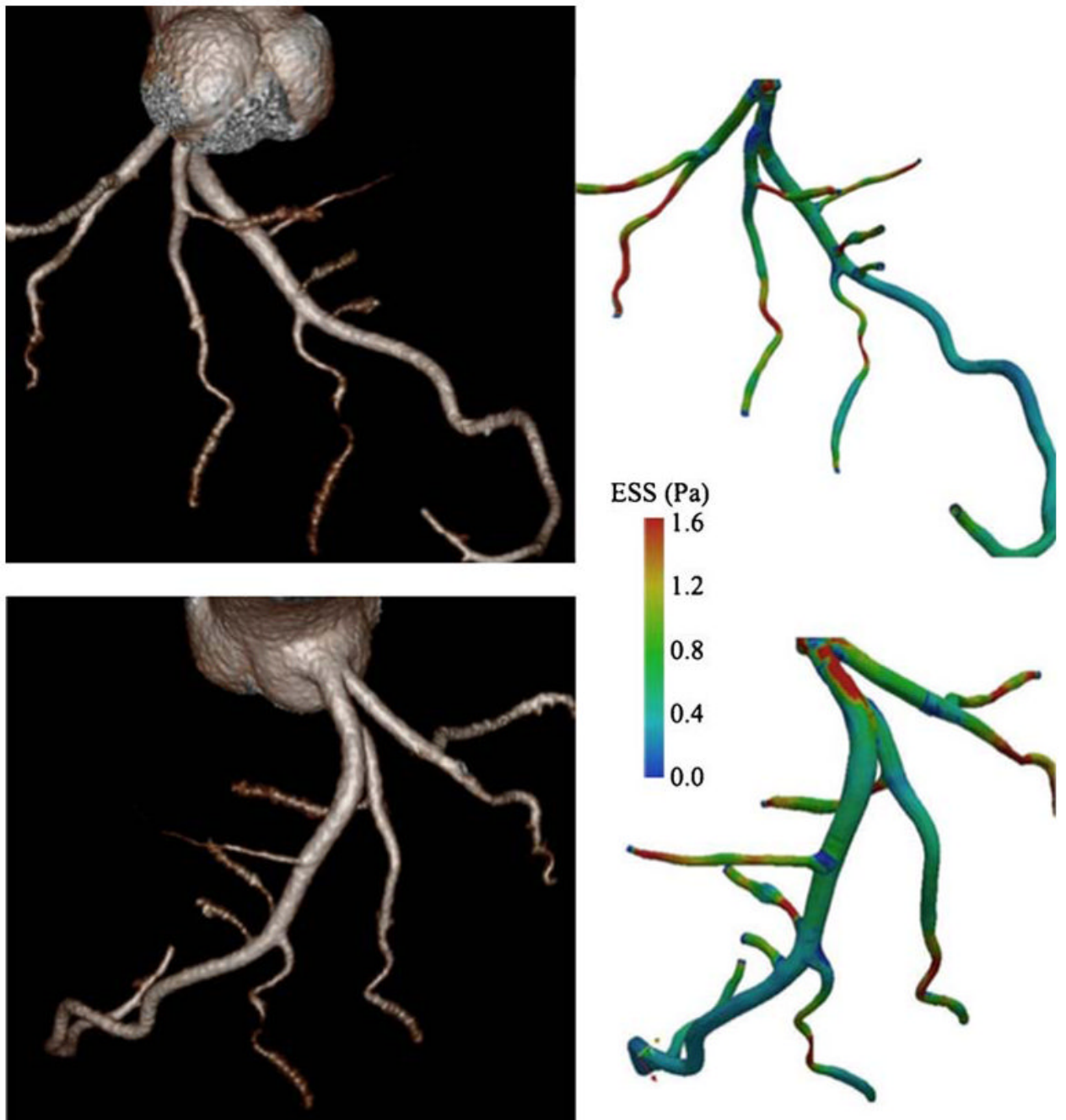
Fig. 1.
Whole intracoronary endothelial shear stress (ESS) mapping from single-heartbeat 320-detector row CT (Toshiba Aquilion One Dynamic Volume CT; Tochigi, Japan) after injection of 80 mL of iopamidol, 370 mg I/mL (Isovue-370; Bracco Diagnostics, Princeton, NJ), followed by 40 mL of normal saline injected with a dual injector (EZEM Empower CTA DUAL Injector; EZEM Inc., Lake Success, NY). Three-dimensional volume-rendered images generated from Vitrea 4.1 software (Vital Images, Minnetonka, MN) (*left side*). Corresponding ESS maps (*right side*). Simulated blood flow uses a computational fluid dynamic technique. (*Adapted from* Ramkumar et al. [59]; with permission)